Korean Journal of Remote Sensing, Vol.22, No.1, 2006, pp.49~61

A Fast Processing Algorithm for Lidar Data Compression Using Second Generation Wavelets

B. Pradhan*†, K. Sandeep, Shattri Mansor*, Abdul Rahman Ramli*, and Abdul Rashid B. Mohamed Sharif***

Institute for Advanced Technologies (ITMA), Faculty of Engineering, University Putra Malaysia, 43400, UPM, Serdang, Selangor Darul Ehsan, Malaysia*

Department of Mechanical Engineering, Institute of Technology, Banaras Hindu University (BHU), Varanasi, 22105, Uttar Pradesh, India**

Abstract : The lifting scheme has been found to be a flexible method for constructing scalar wavelets with desirable properties. In this paper, it is extended to the LIDAR data compression. A newly developed data compression approach to approximate the LIDAR surface with a series of non-overlapping triangles has been presented. Generally a Triangulated Irregular Networks (TIN) are the most common form of digital surface model that consists of elevation values with x, y coordinates that make up triangles. But over the years the TIN data representation has become an important research topic for many researchers due its large data size. Compression of TIN is needed for efficient management of large data and good surface visualization. This approach covers following steps: First, by using a Delaunay triangulation, an efficient algorithm is developed to generate TIN, which forms the terrain from an arbitrary set of data. A new interpolation wavelet filter for TIN has been applied in two steps, namely splitting and elevation. In the splitting step, a triangle has been divided into several sub-triangles and the elevation step has been used to 'modify' the point values (point coordinates for geometry) after the splitting. Then, this data set is compressed at the desired locations by using second generation wavelets. The quality of geographical surface representation after using proposed technique is compared with the original LIDAR data. The results show that this method can be used for significant reduction of data set.

Key Words : Light Detection and Ranging (LIDAR), Delaunay Triangulation, Triangulated Irregular Network (TIN), Geographical Information System, Lifting scheme, Second generation wavelet, Image compression.

1. Introduction

Large digital terrain data sets such as Light Detection and Ranging data (LIDAR) are used in Geographic Information System (GIS) applications. The storage, transmission and visualization of terrain data pose challenges for its use in GIS and potential applications on the World Wide Web. A compression technique is needed for this terrain data, because transmitting terrain data is crucial to a web-based GIS.

Received 17 October 2005; Accepted 13 February 2006.

† Corresponding Author: B. Pradhan (biswajeet@mailcity.com)

Research on GIS data compression for managing large data sets dated back to 1980s. Recently, most of the methods for image (spatial data) compression are based on wavelets and related techniques. Most of the commercial exisiting image compression software is based on the first generation wavelets. Very little work has been done on image compression based on second generation wavelets (Amaratunga *et. al.*, 2003). Wavelet approaches for image compression tend to outperform Fourier approaches because of its ability to represent both spatially localized features and smooth regions in an image. The superior compression capability of wavelets combined with their natural multiresolution structure makes them a good representation for storing images. While working with dyadic wavelet decomposition digital images are represented by wavelet coefficients. These types of representation in dyadic wavelet decomposition are known as linear decomposition over a fixed orthogonal basis. The non-linearity in the approximation of images by wavelets is introduced by the thresholding of the wavelet coefficients. This type of approximation can be viewed as mildly nonlinear. Recently, several highly nonlinear methods for capturing the geometry of images were developed, such as wedgelets (Donoho, 1999); as well as edge-adapted nonlinear multiresolution and geometric spline approximation (Demaret *et al.*, 2004).

This paper presents a new approach for LIDAR data compression method using second generation wavelets. A random set of points has been approximated to represent a surface by Delaunay triangulation. The theory, computations, and applications of Delaunay triangulations and Voronoi diagrams have been described in detail in the literature (Lawson, 1972; Sibson, 1978; Lee and Scachter, 1980; Watson, 1981; Mirante and Weingarten, 1982; Macedonio and Pareschi, 1991; Kao *et al.*, 1991; Puppo *et al.*, 1992; Tsai, 1991, 1993). The present work describes a fast algorithm based on Tsai's Convex Hull Insertion algorithm (Tsai, 1991, 1993), for the construction of Delaunay triangulations of arbitrary collections of points on the Euclidean plane. The original algorithm has been improved further for a faster computation of geometric structures. The source code has been written in FORTRAN compiler. Once the triangulated irregular network has been created from the random set of points was further subjected to compression by using second generation wavelets. Results were shown in a comparative study basis for the TIN data compression at different level of resolution.

2. Delaunay Triangulation

Many researchers (Lawson, 1972; Evans *et al.*, 2001; Abásolo, *et al.*, 2000) have suggested different ways to construct triangulations with the local equilateral property. A well known construction called the Delaunay Triangulation simultaneously optimizes several of the quality measures such as max-min angle, min-max circumcircle, and min-max min-containment circle. Jünger and Snoeyinks (1998) have proposed Delaunay triangulation for progressive visualization. The Delaunay triangulation "DT" of a point set is the planar dual of the famous Voronoi diagram. The Voronoi diagram is a partition of the plane into polygonal cells one for each input point so that the cell for input point 'a' consists of the region of the plane closer to 'a' than to any other input point. So long as no four points lie on a common circle then each vertex of the Voronoi diagram has degree three and the DT which has a bounded face for each Voronoi vertex and vice versa will indeed is a triangulation. If four or more points do lie on a common circle then these points will be the vertices of a larger face that may then be triangulated to give a triangulation containing the DT Voronoi diagrams and

Delaunay triangulations have been generalized in numerous directions. There is a nice relationship between Delaunay triangulation and three dimensional convex hulls by lifting each point of the input to a paraboloid in three-space by mapping the point with coordinates (x, y) to the point (x, y, $x^2 + y^2$). The convex hull of the lifted points can be divided into lower and upper parts: a face belongs to the lower convex hull if it is supported by a plane that separates the point set from (0, 0, - ∞). It can be shown that the DT of the input points is the projection of the lower convex hull onto the -plane as depicted in Figure 1. Finally a direct characterization: if and are input points the DT contains the edge {a, b} if and only if there is a circle through and that intersects no other input points and contains no input points in its interior. Moreover each circumscribing circle (circumcircle) of a DT triangle contains no input points in its interior.

The following are some properties of Delaunay triangulations have been discussed.

Let Y denote a finite planar point set.

- A Delaunay triangulations D(Y) of is one, such that for any triangle in D(Y), the interior of its circumcircle does not contain any point from Y. This specific property is termed as Delaunay property.
- The Delaunay triangulation D(Y) of Y is unique, provided that no four points in Y are co-circular. Since neither the set X of pixels nor its subsets

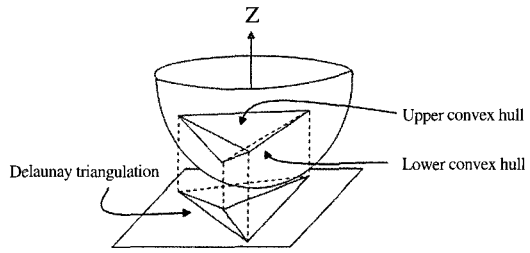

Figure 1. The lifting transformation maps the DT to the lower convex hull.

satisfy this condition, we initially perturb the pixel positions in order to guarantee unicity of the Delaunay triangulations of X and of its subsets. Each perturbed pixel corresponds to one unique unperturbed pixel.

For any y∈Y, D(Y\y)can be computed from D(Y) by a local update. This follows from the Delaunay property, which implies that only the cell C(y) of y in D(Y) needs to be retriangulated. Recall that the cell C(y) of y is the domain consisting of all triangles in D(Y) which contain as a vertex. Figure 1 shows a vertex y∈D(Y) and the Delaunay triangulation of its cell C(y).

D(Y) provides a partitioning of the convex hull [Y] of Y. Figure 2 shows the irregular set of 12 points and Figure 3 shows the Delaunay triangulation of these points.

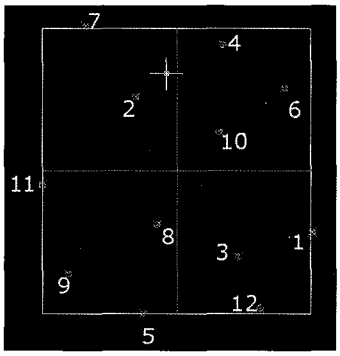

Figure 2. It shows Irregular set of points.

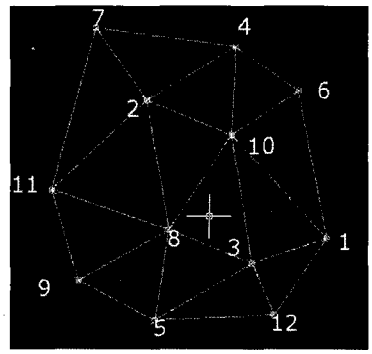

Figure 3. It shows the TIN data structure using Delaunay triangulation.

3. Interpolation Wavelet Filters for TIN

The lifting scheme is a tool for constructing second-generation wavelets (Sweldens, 1994, 1997), which are no longer, dilates and translates of one single function. Donoho (1993) have also undertaken related work on second generation wavelets. In contrast to first-generation wavelets, which used the Fourier transform for wavelet construction, a construction using lifting is performed exclusively in spatial domain and, thus, wavelets can be custom designed for complex domains and irregular sampling.

The basic idea behind lifting is to start with simple multiresolution analysis and gradually build a multiresolution analysis with specific, a priori defined properties. The lifting scheme can be viewed as a process of taking an existing wavelet and modifying it by adding linear combinations of the scaling function at the same level of resolution.

An interpolation wavelet filter for TIN lies in subdivision process which has two steps (Kiema and Bahr, 2001). One is a splitting step; the other one is an elevation step. In the splitting step, a triangle is divided into several sub-triangles (Wu and Amaratunga, 2003; Dyn *et al.*, 1990; Cohen, 2001). The elevation step is to calculate the point values (point coordinates for geometry) after the splitting. Let us discuss this partition step mathematically.

Let us consider a surface as represented in Figure 4 and Figure 5 can be defined mathematically as:

$$\text{Surface } S_n = \{S_{n,j} \mid 0 \le j < 2^n\} \quad (1)$$

The surface value at $x_{n,j}$ can be spiltted into two sets of coefficients as shown in equation 3 and 4. Figure 6 shows the wiring diagram of spiltting, predicting and updating steps of the surface. The surface is spiltted into even and odd set of coefficients as seen in Figure 7.

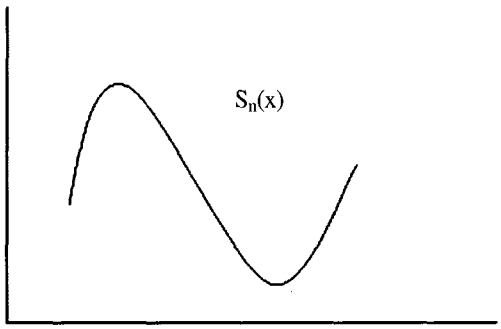

Figure 4. It shows graphical representation of surface.

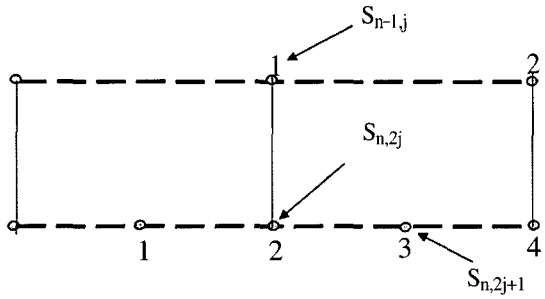

Figure 5. It shows mathematical representation of surface.

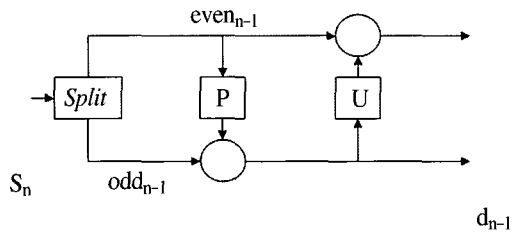

Figure 6. It shows the wiring diagram for spilting, predicting and updating steps for lifting scheme.

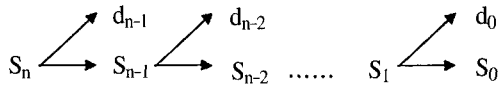

Figure 7. It shows the schematic diagram for spiltting step.

$S_{n,j}$: surface value at $x_{n,j}$

$$(even_{n-1}, odd_{n-1}) = split(S_n) \quad (2)$$

$$Sn = \{S_{n,0}, S_{n,1}, S_{n,2}, S_{n,3}, S_{n,4}, S_{n,5}, S_{n,6}, S_{n,7}\}$$

$$even_{n-1} = \{S_{n,0}, S_{n,2}, S_{n,4}, S_{n,6}\} \quad (3)$$

$$odd_{n-1} = \{S_{n,1}, S_{n,3}, S_{n,5}, S_{n,7}\} \quad (4)$$

In predicting step, even samples can be used to calculate the odd samples and vice versa. In this step, only the even-indexed coefficients of the previous scale are available. Thus to reconstruct the previous scale, we need a predictor to calculate the missing odd-indexed coefficients for the upper scale. This operator may use the correlation which exists between $even_{n-1,2k}$ coefficients. Obviously, some error between the approximated even indexed point, $P(even_{n-1,k})$ and the actual value, $even_{n,2k-1}$ is expected. This error represents the loss of accuracy as we move toward the coarser scale.

$$d_{n-1} = odd_{n-1} - P(even_{n-1}) \quad (5)$$

The construction of prediction operator is based on some model of the data but not on the data itself. The method used here to find a prediction function is called interpolating subdivision (Swelden, 1997). To predict a value for an odd-indexed point, we will construct a polynomial with degree N-1 which passes through even-indexed neighboring points. Depending upon the degree of the polynomial, accuracy of the prediction will be different.

Updating step ensures that the coarse surface have the same average value as the original surface. Therefore a sequence of coefficientshas S_{n-1} to be lifted such that Equation (5) is satisfied. This requirement can be satisfied by using an operator $U(d_{n-1})$ and the $even_{n-1}$ values of the previous scale such that

The update operator can be written as:

$$S_{n-1} = even_{n-1} + U(d_{n-1}) \quad (6)$$

Each d_{n-1} is surrounded by the number of $\tilde{N}$ of the c coefficients. For each d_{n-1} and $\tilde{N}$ neighboring c coefficients, the operator U may have different lifting coefficients. As an example, for $\tilde{N} = 2$ two coefficients a,b can be identified for d_{n-1}. The $S_{n-1,k-1}$, $S_{n-1,k+1}$ are the coefficients which will be lifted. Therefore,

$$\begin{cases} S_{n-1,k-1} = S_{n-1,k-1} + a * d_{n-1,k} \\ S_{n-1,k+1} = S_{n-1,k+1} + b * d_{n-1,k} \end{cases} \quad (7)$$

Where n represents the n^{th} scale and k is the counter for coefficients. At the finest scale, the c coefficients are assumed equal to the sample points.

1) Proposed Lifting Scheme Algorithm

In this section, a new algorithm based on lifting scheme has been proposed. We have derived new sets of equations based on the area of triangle methods as shown in Equation 8 and Equation 11. The LIDAR terrain data has been encoded as a discrete surface, i.e. a finite set of points in three-dimensional (3-D) space, by considering a non-negative discrete function of two variables F(x, y) and establishing the correspondence between the image and the surface $A = \{(x, y, c) | c = F(x, y)\}$, so that each point in corresponds to a pixel in the image; the couple (x, y) gives the pixel's position in the XY plane, while c is the point's height.

Our goal is to approximate A by a discrete surface $B = \{(x, y, d) | d = G(x, y)\}$, defined by means of a finite set of points. Let T be a generic triangle on the XY of vertices:

$$P_1 = (x_1, y_1), P_2 = (x_2, y_2), P_3 = (x_3, y_3)$$
and let
$$c_1 = F(x_1, y_1), c_2 = F(x_2, y_2), c_3 = F(x_3, y_3), \quad (8)$$

Where P_1, P_2 and P_3 are represented as

$(x_1, y_1, c_1), (x_2, y_2, c_2), (x_3, y_3, c_3) \in A$.

Let O be the centroids of the triangle which means a new point after adding into the triangulation as shown in Figure 8. Let A_1, A_2 and A_3 be the area of the three triangles. Then the total area can be represented as:

$$A = A_1 + A_2 + A_3 \quad (9)$$

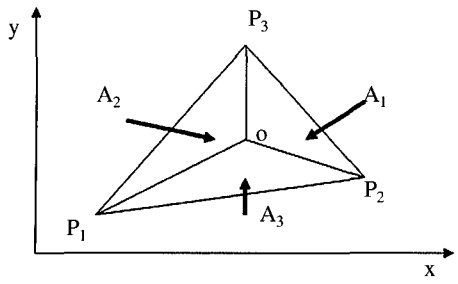

Figure 8. It shows a surface showing the areas of the triangles to calculate the wavelet coefficients.

Now, the detail coefficient can be represented as:

$$d^n = Z^n - P(Z_e^n) \quad (10)$$

Where, d^n is the detail coefficient at the n^{th} level and $P(Z_e^n)$ is the predicted value at n^{th} level and Z^n is the values at the odd samples.

The equation above can be rewritten in a general form for $n-1^{th}$ level as

$$Z^{n-1} = Z^n_{even} + C(d^n) \quad (11)$$

where $C(d^n)$ is the correction factor for wavelet coefficients.

By using the correction factor, "significant points" were identified from the irregular set of data. First, the irregular set of points were taken and used it to find average signal and difference signal (detail coefficients) as described in Equation 10. Delaunay triangulation and bivariate splines are used to estimate average signal and difference signal. High difference signal or detail coefficient value indicates significance of a point. The bivariate splines used to quantize the signal over Delaunay triangulation. The purpose of this work is to find significant points and use only this set of points to represent terrain. The size of this set of significant points has become very small compared to the original data set and hence the data file will be compressed. This data set can be transferred easily and terrain image can be regenerated by using a small program based on Delaunay triangulation and bivariate splines.

The generating process for the LIDAR data compression is as follows:

1. Due to randomly distributed raw data points, the data is interpolated by means of a linear function. It is aiming to enable processing with regularly distributed grid data.
2. Using the Delaunay algorithm the TIN model of the surface has been calculated. For each triangle in the TIN model the coordinates of the vertices and their respective height values of the three points that compose it were calculated.
3. The adjacency matrix that formed by the bounded edges for all triangles has been calculated.
4. The coordinates of the vertices and triangle edges has been rewritten in WTIN data structure.
5. The wavelet filter for each triangle has been calculated based on the area method as described in Equation 11. Wavelet coefficients have been determined to check and compare the area of each triangle based on lifting scheme. If the wavelet coefficient value is much higher than the threshold value then vertices were retained. If the difference falls below a predefined threshold the original points are selected. This process is completed with the number points added during the presented iteration and was continued till all the points were checked.
6. By using iterative processing, the original LIDAR points were compared with the compressed data and their respective Peak Signal to Noise Ratio (PSNR) values were calculated for both images to compare the compression ratio.

4. Experimental Results

All algorithms were coded in Visual Fortran and

MATLAB and executed on a Pentium IV, 256 MB RAM machine. The optimized code is about 2000 lines of Visual Fortran and 500 lines of MATLAB. To evaluate the performance of the wavelet based triangulation compression method several test data were used. The wavelet based triangulation compression method gives consistently better performance for the LIDAR data that we used. This section presents some results of the algorithm on LIDAR data using the wavelet based triangulation compression method at different levels of quality.

In our test, at each recursion step about 25% of the vertices are removed by using the second generation wavelet and lifting scheme. The number of triangles in the hierarchy is at most only three times larger than the number of triangles of the initial triangulation. We next examine the storage overhead caused by the maintenance of the hierarchy. The total amount of storage in bytes of the data structure described in previous section, which may include multiple copies of the same triangle, is only 4 to 5 times larger than the storage of the initial triangulation. In our implementation, this gave a total memory requirement for the hierarchical representation of a terrain of data points of roughly bytes. The data structure of Delaunay triangulation is different from the data structure of wavelet compression in two ways. First, we no longer store multiple copies of the same triangle, instead we store for each triangle the level at which it was created. Second, we introduce the intermediate nodes, which reduce the total number of pointers in the structure. Together these two changes reduce the storage requirement by one third, which means that the storage is about 3.5 times as much as the storage for the initial terrain.

If the increase in storage would still be too much, it is possible to have a trade-off between the size of the structure and the difference between subsequent levels. In particular, instead of requiring the deleted vertices to form an independent set, we can require that they form independent groups of a certain size.

1) Data Used

Two different sets of LIDAR data were tested using the lifting scheme algorithm to check the efficiency of the compression program. The data were in ASCII format describing the x, y and z values for the points as shown in Figure 9. Delaunay triangulation method for the creation of the TIN has been applied to the original data. A new algorithm has been developed for the creation of the TIN. Further, TIN was compressed using the second generation wavelets. A new algorithm for second generation wavelet compression is proposed. Based on the initial configuration of the original TIN, different resolutions are constructed during wavelet analysis.

In the first step the TIN model for the surface using the Delaunay algorithm has been calculated. This data set is compressed at the desired locations by using second generation wavelets. Figures 10a, Figure 11a and Figure 12a show the view of the LIDAR terrain at three levels and the corresponding triangulations (Figure 10b, Figure 11b and Figure 12b), generated using our compression method. In the Figure 10b it can be noticed that the number of

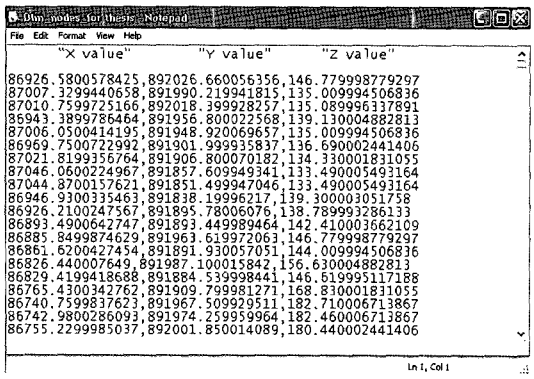

Figure 9. It shows the original LIDAR data in ASCII format.

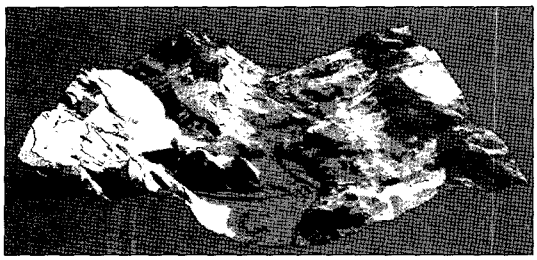

Figure 10a. Initial terrain for first LIDAR data set (Gouraud shaded).

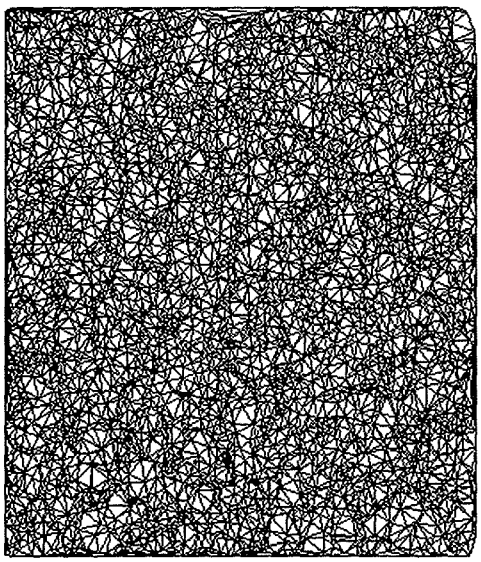

Figure 10b. Triangulation for the initial terrain (5,000 points).

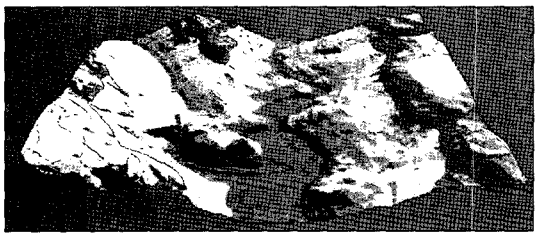

Figure 12a. Terrain compressed at 23% (Gouraud shaded) and its triangulation (870 points).

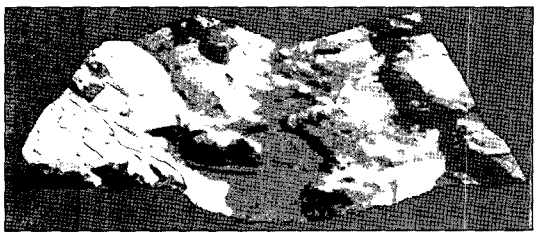

Figure 12c. Terrain compressed at 37%.

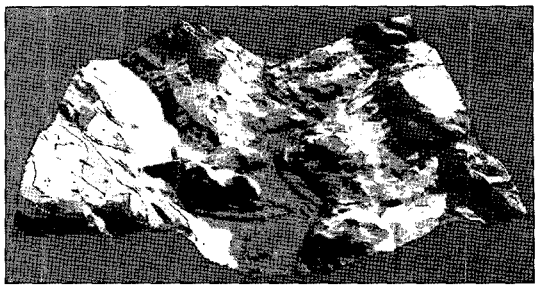

Figure 11a. Terrain compression at 12 %(Gouraud shaded) and its triangulation (1,023 points).

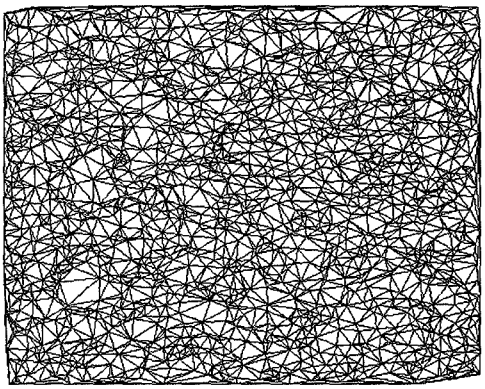

Figure 11b. Triangulation for the terrain at 12% (1,023 points).

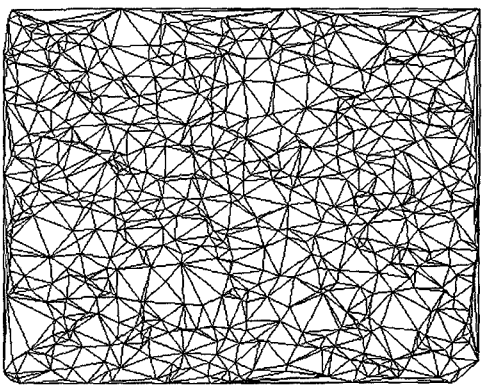

Figure 12b. Triangulation of the terrain at 23% (870 points).

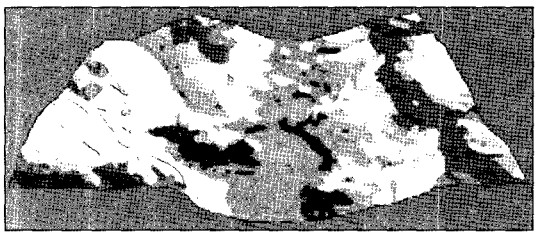

Figure 12d. Terrain compressed at 56%.

triangles have been reduced significantly to reduce the size of the original data. However, while deleting the vertex points, we must be careful not to remove vertices that are very much significant for the generation of surface, such as peaks, pits, and passes. Therefore, the computation needs human intervention to select the number of points desired to be deleted from the hierarchy. Note that the vertices of the convex hull of the data points are always the same, meaning fixed so that the terrain keeps its original size. Figure 13a, Figure 14a and Figure 15a show the view of the second set of LIDAR terrain at different levels and the corresponding triangulations (Figure 13b, Figure 14b and Figure 15b), generated using our compression techniques. The first LIDAR data as shown in Figure 10a has 5,000 points. Figure 10b shows the Delaunay triangulation for the original data computed using the proposed algorithm. Figure 11a shows the result after 12% compression and Figure 11b shows the Delaunay triangulation for the compressed image. Here, the number of "significant points" has been reduced significantly to 1023 number of points. Remaining insignificant points were removed from the data thus reducing the size of the terrain. It can be clearly seen that, there is no change in the quality of the surface after 12% compression. Figure 12a shows the image after 23% compression. Here the numbers of significant points were reduced further to 870 points. Visual observation shows the quality of the surface is still

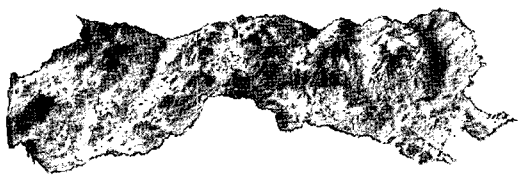

Figure 14a. Terrain compressed for second LIDAR data set at 12% (Gouraud shaded).

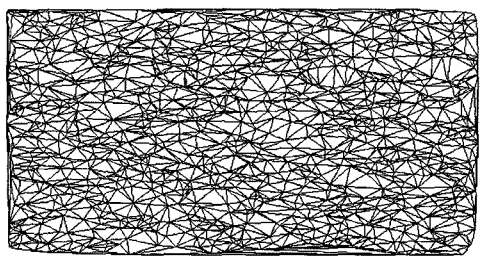

Figure 14b. Triangulation of the terrain at 12% (4812 points).

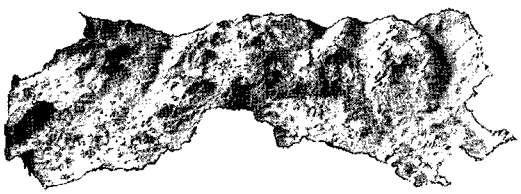

Figure 13a. Initial Terrain for second LIDAR data set (Gouraud shaded).

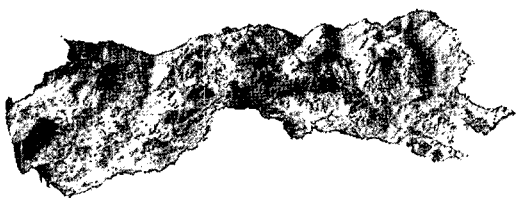

Figure 15a. Terrain compressed for second LIDAR data set at 23% (Gouraud shaded).

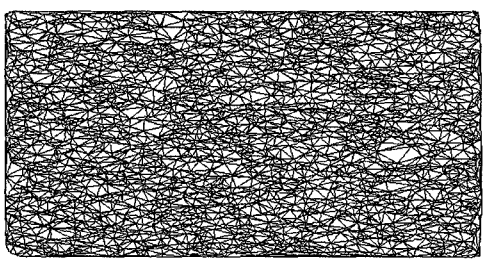

Figure 13b. Triangulation for the initial terrain (9,823 points).

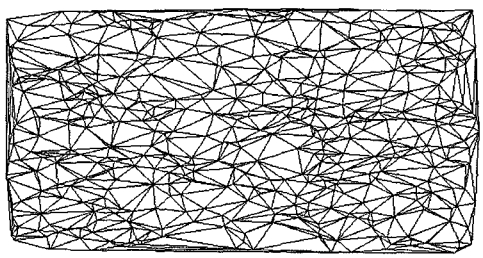

Figure 15b. Triangulation of the terrain at 23% (2391 points).

not changed. However, further compression at 37% and 56%, the quality of the terrain has been degraded as shown in Figure 12c and 12d. It shows that the maximum threshold for the wavelet coefficients has been achieved. The second LIDAR data set that we have used in our compression scheme has 9823 number of points. Figure 13a shows the original LIDAR data set. Figures 14a, 14b and 15a, 15b show the results computed using the wavelet based lifting scheme algorithm. Figure 14a shows the results after 12% compression and figure 15a shows after 23% compression. This work also provides current implementation of wavelet coefficients during the compression operation. The proposed algorithm has the multiresolution capability and easy to compress due to large number of wavelet coefficients with small magnitudes which is suitable for distributed GIS applications such as web displaying.

5. Model Validation and Comparisons with Alternative Methods

Results were evaluated by visual analysis as well as by Peak-Signal-to-Noise Ratio (PSNR) and error image criteria (Slone *et. al.*, 2000). A program was written in MATLAB for PSNR analysis. The Peak Signal to Noise Ratio PSNR (dB) that measures the size of the error relative to the peak value of the signal. In order to obtain quantitative measures an analysis of the gray value histograms has to be performed which can lead to the Peak-Signal-Noise-Ratio (PSNR) which describes the relation between the maximal gray value within the original image (peak) and the noise that is caused through the compression. PSNR is defined as

$$PSNR = 10*\log\left(\frac{peak^2}{noise}\right)$$

Here, noise refers to the Mean Square Error (MSE) as described below.

A widely used measure of reconstructed image for an N x M size image is the mean square error (MSE) as given by:

$$MSE = \frac{1}{n*m}\sum_{i=0}^{n-1}\sum_{j=0}^{m-1}(g_{ij} - g'_{ij})^2$$

Here g_{ij} is the grey value within the original and g'_{ij} the corresponding value within the compressed image (both images of dimension). It is desirable to obtain as less noise as possible and with that a large PSNR value.

For our experiments, mean square error (MSE) and peak signal to noise ratio (PSNR) was applied to check the error of the compressed image. Lifting scheme based wavelet decomposition was applied to the LIDAR images. For each decomposition level, the numbers of significant points are reduced. With various combinations of using different decomposition levels objective measures (PSNR) and subjective measures (MSE) are presented versus compression ratio (CR). In order not to make complicated combinations of various decomposition levels, only one data from the highest decomposition level were kept, i.e. data from the lowest decomposition is always ignored.

Figure 16 shows the average values for PSNR from the differences between the original and the reconstructed images for both LIDAR images under study for three level decompositions. As can be seen, the PSNR and compression ratio values vary

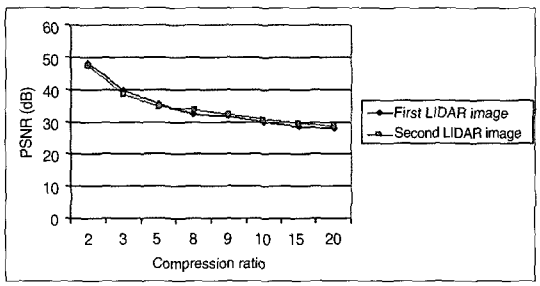

Figure 16. Graph showing relationship between compression ratio and PSNR.

inversely. In several cases we have an instance where PSNR values are not in good accord with visual quality criteria, while in the other cases the visual quality increases as the MSE error goes down. Fig. 12 c and Figure 12d show the images for the first LIDAR image after deleting more number of significant points.

Table 1 shows the test statistics obtained for the first LIDAR image. In Table 1 [insert table 1 about here] the first column specifies the MSE, while the following columns specify the compression ratio, and Peak signal-to-noise ratio (PSNR). Table 2 shows the test result obtained for the second LIDAR image using the same compression ratio. From the analysis of data in Tables 1 and 2, it can be seen that the PSNR ratio decreases with the compression ratio as seen in Figure 16. PSNR value was between 27.98 to 48.24 dB and 28.54 to 47.28 dB for first and second LIDAR images respectively. We tested the algorithm on various types of terrain images from different application domains of LIDAR data; on all these test images similar conclusions can be drawn. Figure 17 shows the comparison between MSE and compression ratio for both images. It can be seen that the trend of the MSE is almost same for both images. The MSE value was between 3 to 10.4 and 4 to 9.8 for first and second images respectively. All these images were compressed and decompressed until 20:1 compression ratio.

In order to assess the effectiveness of our compression algorithm on LIDAR image, four schemes are applied: our lifting scheme based method; JPEG2000; MrSID and ECZ compression methods. Quantitative measurements are used to evaluate the performance of the compression schemes. The result of the compression of PSNR is that JPEG 2000 is 34.62 dB, MrSID is 38.5 dB, ECW is 34.5 dB and lifting scheme based is 39.25 dB, in average. Figure 18 demonstrates the superiority of

Table 1. It shows the test statistics obtained for the first LIDAR image.

MSE	Compression ratio	PSNR
3	2	48.24
4.1	3	39.73
5.21	5	35.54
6.23	6	32.34
7.34	8	31.68
8	10	30
9.1	15	28.59
10.4	20	27.98

Table 2. It shows the error analysis, compression ratio and PSNR values for second LIDAR image.

MSE	Compression ratio	PSNR
1.9	2	47.28
4	3	38.38
6	5	34.56
8	6	33.79
11	8	32.31
13	10	30.76
13.3	15	29.84
13.9	20	28.54

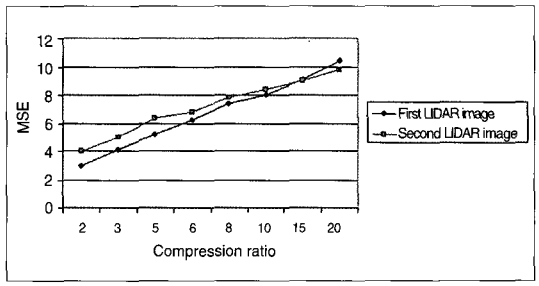

Figure 17. Graph showing relationship between compression ratio and MSE.

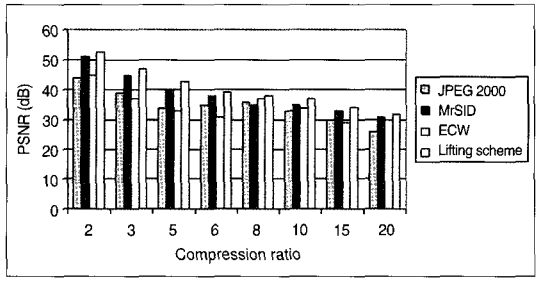

Figure 18. Graph showing comparison with other lifting scheme models against JPEG 2000, ECZ and MrSID.

our method against JPEG with increasing compression ratios and validate the mentioned results of the visual inspection.

6. Conclusion

The construction of Triangulated Irregular Network using Delaunay triangulation for the LIDAR data has been shown. This approach uses fast and efficient second generation wavelets algorithm for multiresolution analysis of GIS data compression. This algorithm is easy to perform the mathematical and computational operation with minimal time, irrespective of the large data. Our algorithm scheme preserves high-gradient regions that might exist in a given data set. We have tested our method with various data sets. The computational cost of our algorithm depends on the different approaches used. The initial triangulation can be done in O (nlogn), the gradient approximation can be done in O (nlogn). The individual refinement step has to check all the original data points lying in the involved triangles, so the complexity of each step is O(n). How often the iteration step is executed depends on the error value given in the input. As a general rule, the authors have assumed that no more iteration should be done than they are original data sites. So the overall complexity is $O(n^2)$.

Acknowledgments

Authors would like to thank various anonymous reviewers for their useful comments to bring the paper into the present form.

References

Abásolo, M. J., Blat, J., and De Giusti, A., 2000. A Hierarchial Tringulation for Multiresolution Terrain Models. *The Journal of Computer Science & Technology (JCS&T)*, 1, 3

Cohen, A., 2001. Applied and computational aspects of nonlinear wavelet approximation, *Multivariate Approximation and Applications*, N. Dyn, D. Leviatan, D. Levin, and A. Pinkus (eds.), Cambridge University Press, Cambridge, pp. 188-212.

Demaret, L., Dyn, N., Floater, M. S., and Iske, A., 2004. Adaptive thinning for terrain modelling and image compression, in *Advances in Multiresolution for Geometric Modelling*, N. A. Dodgson, M. S. Floater, and M. A. Sabin (eds.), Springer-Verlag, Heidelberg, pp. 321-340.

Donoho, D., 1999. Wedgelets: nearly-minimax estimation of edges, *Annals of Stat.*, 27: 859-897.

Dyn, N., Levin, D., and Gregory, J. A., 1990. A butterfly subdivision scheme for surface interpolation with tension control, *ACM Transaction on Graphics*, 9: 160- 169.

Evans, W., Kirkpatrick, D., and Townsend, G., 2001. Right-Tringulated Irregular Networks. Algorithmica, *Special Issue on Algorithms for Geographical Information Systems*, 30(2): 264-286.

Jünger, B. and Snoeyink, J., 1998. Selecting independent sets for terrain simplification. *Proceedings of WSCG '98*, Plzen, Czech Republic, February 1998, University of West Bohemia, pp. 157-164.

Kao, T., Mount, D. M., and Saalfeld, A., 1991. Dynamic maintenance of Delaunay triangulations: *Proc.*

Auto-Carto 10, Baltimore, Maryland, p. 219-233.

Kiema, J. B. K. and Bahr, H.-P., 2001. Wavelet compression and the automatic classification of urban environments using high resolution multispectral imagery and laser scanning data, *Geoinformatics*, 5: 165-179.

Lawson, C. L., 1972. Generation of a triangular grid with application to contour plotting, California Institute of Technology, Jet Pollution Laboratory, Technical Memorandum No. 299.

Lee, D. T. and Schachter, B. J., 1980. Two algorithms for constructing a Delaunay triangulation, *Intern. Jour. Computer and Information Sciences*, 9(3): 219-242.

Macedonio, G. and Pareschi, M. T., 1991. An algorithm for the triangulation of arbitrary distributed points: applications to volume estimate and terrain fitting, *Computers & Geosciences*, 17(7): 859-874.

Mirante, A. and Weingarten, N., 1982. The radial sweep algorithm for constructing triangulated irregular networks, *IEEE Computer Graphics and Applications*, 2(3): 11-21.

Puppo, E., Davis, L., DeMenthon, D., and Teng, Y. A., 1992. Parallel terrain triangulation, *Proc. 5th Intern. Symposium on Spatial Data Handling*, v. 2, Charleston, South Carolina, p. 632-641.

Sibson, R., 1978. Locally equiangular triangulations, *Computer Jour.*, 21(3): 243-245.

Slone, R., Foos, D., and Whiting, B., 2000. Assessment of visually lossless irreversible image compression: comparison of three methods by using an image comparison workstation, *Radiology*, 215: 543-553.

Sweldens, W., 1994. Construction and Applications of wavelets in Numerical Analysis, Unpublished PhD thesis, Dept. of Computer Science, Katholieke Universiteit Leuven, Belgium.

Sweldens, W., 1997. The lifting scheme: a construction of second generation wavelets, *SIAM Journal on Mathematical Analysis*, 29: 511-546.

Tsai, V. J. D. and Vonderohe, A. P., 1991. A generalized algorithm for the construction of Delaunay triangulations in Euclidean n-space, *Proc. GIS/LIS '91, v. 2,* Atlanta, Georgia, p. 562-571.

Tsai,V. J. D., 1993. Fast topological construction of Delaunay triangulations and Voronoi diagrams, *Computer & Geosciences*, 19(10): 1463-1474.

Watson, D. F., 1981. Computing the n-dimensional Delaunay tessellation with application to Voronoi polytopes, *Computer Jour.*, 24(2): 167-172.

Wu, J. and Amaratunga, K., 2003. Wavelet triangulated irregular networks, *International Journal of Geographical Science*, 17(3): 273- 289.